Quantifying Anti-Gravity Torques for the Design of a Powered Exoskeleton

Daniel Ragonesi, Sunil K. Agrawal, *Member, IEEE*, Whitney Sample, and Tariq Rahman

***Abstract*—Designing an upper extremity exoskeleton for people with arm weakness requires knowledge of the joint torques due to gravity and joint stiffness, as well as, active residual force capabilities of users. The objective of this research paper is to describe the characteristics of the upper limb of children with upper limb impairment. This paper describes the experimental measurements of the torque on the upper limb due to gravity and joint stiffness of three groups of subjects: able-bodied adults, able-bodied children, and children with neuromuscular disabilities. The experiment involves moving the arm to various positions in the sagittal plane and measuring the resultant force at the forearm. This force is then converted to torques at the elbow and shoulder. These data are compared to a two-link lumped mass model based on anthropomorphic data. Results show that the torques based on anthropometry deviate from experimentally measured torques as the arm goes through the range. Subjects with disabilities also maximally pushed and pulled against the force sensor to measure maximum strength as a function of arm orientation. For all subjects, the maximum voluntary applied torque at the shoulder and elbow in the sagittal plane was found to be lower than gravity torques throughout the disabled subjects' range of motion. This experiment informs designers of upper limb orthoses on the contribution of passive human joint torques due to gravity and joint stiffness and the strength capability of targeted users.**

***Index Terms*— Biomechanics, medical control systems, rehabilitation robotics.**

Fig. 1. Children wearing two versions of the passive WREX. Figure on left shows the WREX attached to a wheelchair, and figure on right shows attached to a body jacket for kids that are ambulatory.

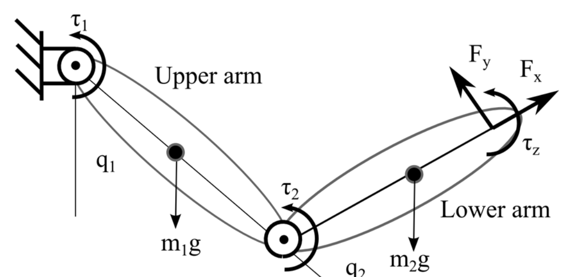

Fig. 2. Model of upper limb as two rigid links with given variables. The symbols q_1 and q_2 are the shoulder and elbow angles, τ_1 and τ_2 are joint torques, $m_1 g$ and $m_2 g$ are the gravity forces, and F_x, F_y, and τ_2 are the measured forces and torque between the human and the measuring device. The force sensor is located at the origin of the force vectors.

I. Introduction

When designing devices that physically interact with humans, it is often necessary to have a model of the human to properly regulate the desired interaction. It is beneficial if the model of the human can be scaled between users based on simple measurements such as height and weight, because it can be time intensive to measure all of the properties for each subject. When the subjects have limited strength, as in this study, the model needs to be accurate enough to be used to detect the user's intention. This paper investigates the biomechanics of a subset of pediatric patients with limited strength, to determine if a generic model can be constructed for the use in a powered upper extremity orthosis that assists people with muscular weakness to perform activities of daily living. A passive arm exoskeleton has already been developed and commercialized by this group [1], [2]. The device is called the Wilmington Robotic Exoskeleton (WREX), which is a gravity-balanced upper limb orthosis for children with muscular weakness present in conditions such as muscular dystrophy (MD) and spinal muscular atrophy (SMA). The WREX has four degrees-of-freedom to allow full range of motion and is assisted by gravity-balancing elastic bands [2]. The WREX can be attached to a wheelchair or to a body jacket. A picture of a currently passive WREX is shown in Fig. 1.

The WREX is designed to counter balance the gravitational load of the arm. Hitherto, the arm was assumed to be simple rods with pinned joints and negligible joint resistance. The current study was undertaken to determine how accurate that assumption is. What are the passive forces in the sagittal plane for people with neuromuscular disabilities and how different are they from those of people without disabilities? This information will determine exactly how much contribution from a powered

Manuscript received November 14, 2011; revised April 18, 2012, July 13, 2012, and August 14, 2012; accepted September 16, 2012. Date of publication October 18, 2012; date of current version March 07, 2013. This work was supported by Nemours Biomedical Research.

D. Ragonesi is with the Department of Mechanical Engineering, University of Delaware, Newark, DE 19716 USA (e-mail: ragonesi@udel.edu).

S. K. Agrawal is with the Department of Mechanical Engineering, Columbia University, New York, NY 10027 USA (e-mail: sunil.agrawal@columbia.edu).

W. Sample and T. Rahman are with the Pediatric Engineering Research Lab, Nemours Biomedical Research, Alfred I. duPont Hospital for Children, Wilmington, DE 19899 USA (e-mail: sample@asel.udel.edu; trahman@nemours.org).

Digital Object Identifier 10.1109/TNSRE.2012.2222047

TABLE I
SUBJECT GROUPS

	Adult	Children	Children with Disabilities
Number of Subjects (N)	5	5	5
Age (yr)	$25-50$	$13-19$	$13-18$
Condition	Normal	Normal	SMA, MD, Arthrogryposis

TABLE II
COEFFICIENTS FOR THE BEST-FIT, THIRD-DEGREE POLYNOMIAL OF NORMALIZED JOINT TORQUES

	Adult		Typical Children		All Typical	
	Shoulder	Elbow	Shoulder	Elbow	Shoulder	Elbow
p_{00}	-0.000992	-0.00401	-0.00420	-0.000513	-0.00259	-0.00226
p_{10}	0.000510	0.000149	0.000467	4.41×10^{-5}	0.000488	9.66×10^{-5}
p_{01}	0.000128	0.000314	0.000219	0.000148	0.000173	0.000231
p_{20}	-3.43×10^{-6}	-1.08×10^{-6}	-2.67×10^{-6}	-1.41×10^{-7}	-3.05×10^{-6}	-6.13×10^{-7}
p_{11}	-2.79×10^{-6}	-2.77×10^{-6}	-3.09×10^{-6}	-5.35×10^{-7}	-2.94×10^{-6}	-1.65×10^{-6}
p_{02}	-1.14×10^{-6}	-3.18×10^{-6}	-2.29×10^{-6}	-1.33×10^{-6}	-1.71×10^{-6}	-2.25×10^{-6}
p_{30}	4.50×10^{-9}	2.25×10^{-9}	1.56×10^{-9}	-3.65×10^{-10}	3.03×10^{-9}	9.43×10^{-10}
p_{21}	1.14×10^{-8}	7.11×10^{-9}	1.24×10^{-8}	-6.55×10^{-10}	1.19×10^{-8}	3.22×10^{-9}
p_{12}	1.14×10^{-8}	8.62×10^{-9}	8.83×10^{-9}	3.66×10^{-10}	7.62×10^{-9}	4.49×10^{-9}
p_{03}	6.40×10^{-9}	1.00×10^{-8}	7.63×10^{-9}	3.57×10^{-9}	5.05×10^{-9}	6.82×10^{-9}

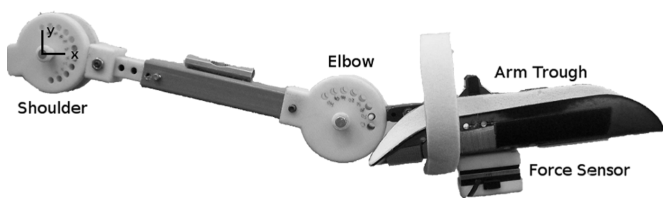

Fig. 3. Measuring device with lockable joints at the shoulder and elbow with a force sensor attached to the arm trough. The subjects forearm is strapped to the arm trough and locked at various positions.

exoskeleton is required. Of particular importance is the proper characterization of the passive joint torques at the human elbow and shoulder.

Much work has been done to model the human upper arm [3]–[5]. In particular, several studies have created models for humans interacting with exoskeletons [6]–[8]. However, these models are for normal subjects and do not account for altered biomechanics of people with neuromuscular disease. This paper summarizes a series of experiments to measure the passive static joint torques and maximum active joint torques a person with a disability can apply through the range of vertical motion. Some work in modeling various disabilities, particularly those of interest to this study, namely SMA, arthrogryposis, and MD, was completed previously. Modeling has been done on the shoulder of patients with tetraplegia [9]. Work has been done on elbow joint properties in Duchenne muscular dystrophy [10], as well as investigating electromyographic activity as it relates to upper limb movement in MD [11]. One group investigated the differences in gait between patients with SMA and MD [12]. Sunnegardh *et al.* investigated the strength of normal children aged 8 and 13 [13]. Mathur *et al.* studied the time-dependent linear decrease in muscular strength of subjects with Duchenne muscular dystrophy [14]. However, the results of these studies are not sufficient to model a subject for control of an upper limb exoskeleton. Therefore, this study was conducted to obtain a preliminary understanding of differences between upper limb

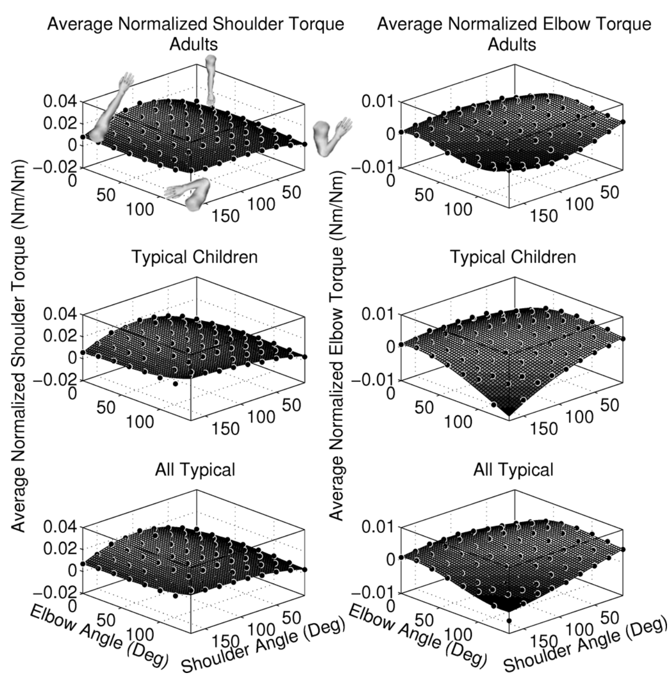

Fig. 4. Average joint torques normalized to subjects' weight and arm length. The arm figures in the upper left graph represent the arm configuration of each section of the graph. The left column is for the shoulder and the right column is for the elbow. The top two graphs are for adults, middle two for children, and bottom two for both groups combined. The dots are data points. The surface is the best fit polynomial.

properties between adults, healthy children, and children with SMA, arthrogryposis, and MD. The end goal is to obtain a robust model that can be used to control a powered assistive device. The controller proposed for our powered orthosis uses residual force input from the user as a measure of his or her intention. The force sensor measures the gravitational load as well as the voluntary force of the user. The ratio of voluntary to gravitation force is very small for weak individuals; therefore, it becomes

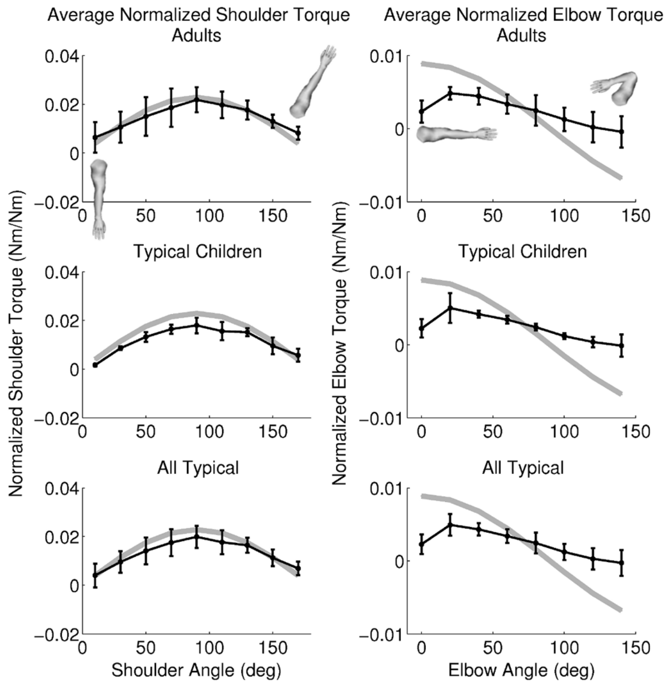

Fig. 5. Cross section of average joint torques normalized to subjects' weight and arm length. Left column is with the elbow locked at 0°. The right column is with the shoulder locked at 90°. The arm figures provide visual representation of the arm orientation. The grey line is the torque expected from the two link lump mass model.

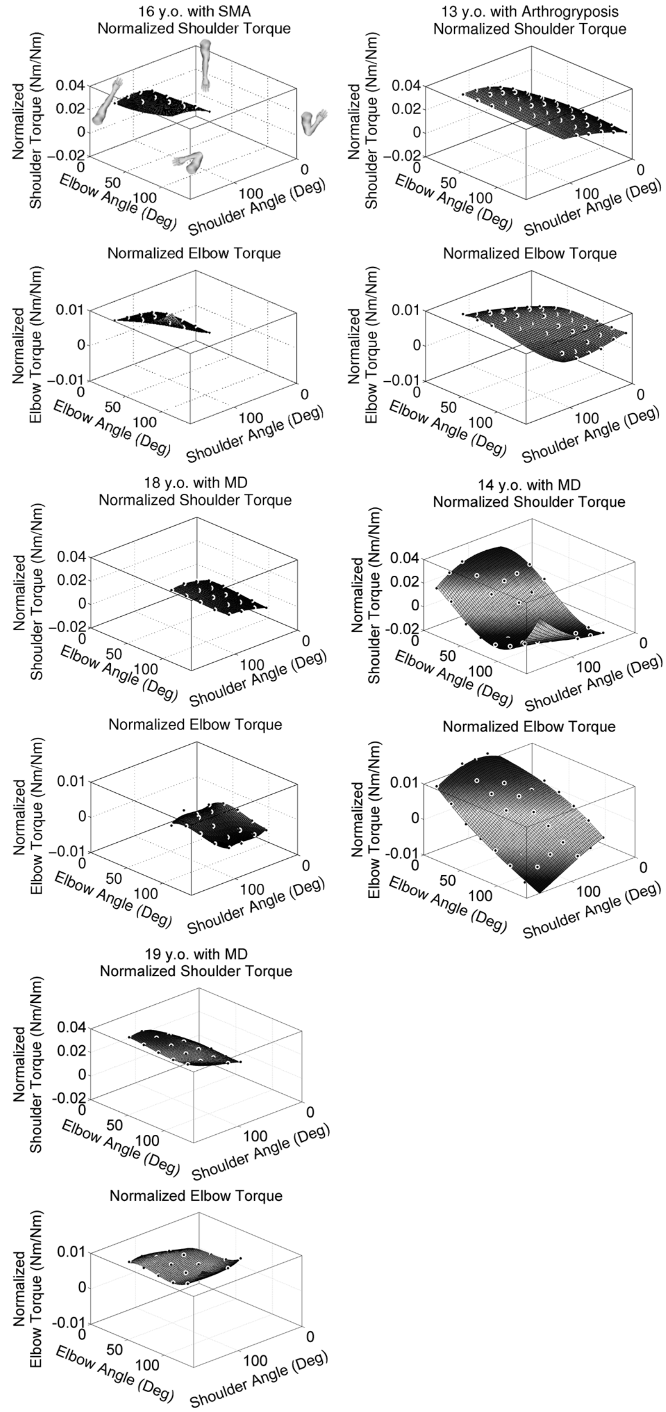

Fig. 6. Normalized joint torques due to gravity of children with disabilities. For each subject the top graph is for the shoulder and the bottom graph is for the elbow.

important to accurately characterize the passive forces (gravitational and passive joint resistances) to better measure the voluntary component. The anthropomorphic model used in this study is based on a person's height and weight and only applies to people without disabilities [15]. Once a general pattern of passive joint torques for people with neuromuscular disabilities is determined, it can be used to modify the torques derived from anthropometry.

II. Joint Torque Measurements

A. Human Model

The initial model for the human arm was a two-link lumped mass model with pin joints shown in Fig. 2. The model was limited to the sagittal plane. The sagittal plane is the only plane where the WREX provides assistance. The other two joints act in the horizontal plane and are passive. Values for segment mass and center of mass were obtained from anthropomorphic tables based on the subject's height, weight, and limb segment lengths [15]. However, initial testing showed that this model was not accurate compared with experimental values. Therefore, the shoulder and elbow joint torques in the vertical plane were measured to quantify that difference.

B. Experimental Protocol

The procedure was approved by the Nemours Institutional Review Board. Consent forms were obtained from all subjects over the age of 18 years. Assent forms were obtained from subjects less than 18 years along with parental permission. The subjects were divided into three groups. Each group had five subjects. This institution treats patients less than 21 years of age; therefore, for the purpose of this study they are put into one group. The three groups were: 1) normal adults over the age of 21 years with no disability of the upper limb, 2) typically developing children aged 7–21 years with no disability of the upper limb, 3) children aged 7–21 years with either MD, SMA, or arthrogryposis. Table I summarizes the three subject categories. For each subject, several body measurements were taken, including height, weight, upper arm length, and lower arm length.

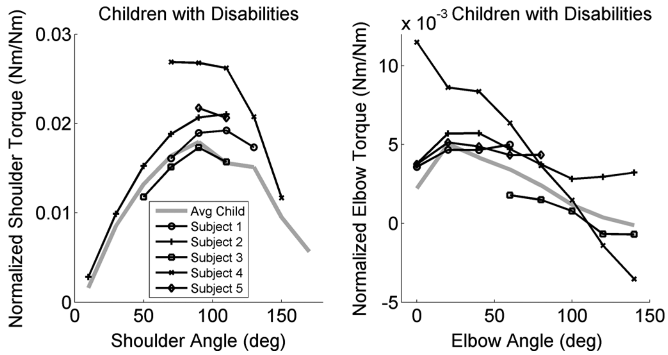

Fig. 7. Cross section of passive joint torques normalized to subjects weight and arm length. The typical children are averaged and shown as a solid line. Each disabled child is shown separately and subject number corresponds to Table III.

The measuring device is shown in Fig. 3. It has two adjustable links with lockable shoulder and elbow joints in 20° increments. An arm trough is connected to a 6-axis force/torque sensor (ATI, Apex, NC, USA). Only the two force directions and one moment direction that act in the vertical plane were recorded. A wrist splint attaches the subject's arm to the device.

The measuring device was adjusted to fit the subject, who sat in a chair or in a powered wheelchair. The subject's forearm was attached to the trough using a wrist splint with Velcro straps. The subject's dominant arm was used in the experiment, since the WREX is typically used on this side. The device was locked at a maximum of nine shoulder joint positions from 10° to 150° from the vertical in 20° increments and eight elbow joint positions from 0° to 140° relative to the upper arm in 20° increments. This gives a total of 72 arm postures. For subjects with disabilities, the number of postures was reduced to remain within the comfortable range of the subject. At each position, a reading from the force sensor was taken. This reading included two forces along the x and y axis and a moment about the z axis. The subject was instructed to relax to prevent misreadings from voluntary muscle activation and were reminded to relax periodically throughout the experiment.

The measured force was transformed into joint torques at the shoulder and elbow using the Jacobian transform

$$\begin{bmatrix}\tau_{\text{shoulder}}\\ \tau_{\text{elbow}}\end{bmatrix} = \begin{bmatrix} a_1\sin(q_2) & a_2 + a_1\cos(q_2) & 1\\ 0 & a_2 & 1\end{bmatrix}\begin{bmatrix}F_x\\ F_y\\ \tau_z\end{bmatrix} \tag{1}$$

where a_1 is the length of the upper arm and a_2 is the length from the elbow to the force sensor.

For the gravitational torques of normal adults, children, and disabled subjects, the joint torques were normalized by dividing a subject's torques by the product of the subject's weight (N) and arm length (m)

$$\tau_{\text{normalized}} = \frac{\tau_{\text{measured}}}{\text{weight} * \text{arm length}}. \tag{2}$$

A third-degree polynomial was fit to the normalized data for both the adults and healthy children

$$\tau(q_1,q_2) = p_{00} + p_{10}q_1 + p_{01}q_2 + p_{20}q_1^2 + p_{11}q_1q_2 + p_{02}q_2^2 + p_{30}q_1^3 + p_{21}q_1^2q_2 + p_{12}q_1q_2^2 + p_{03}q_2^3 \tag{3}$$

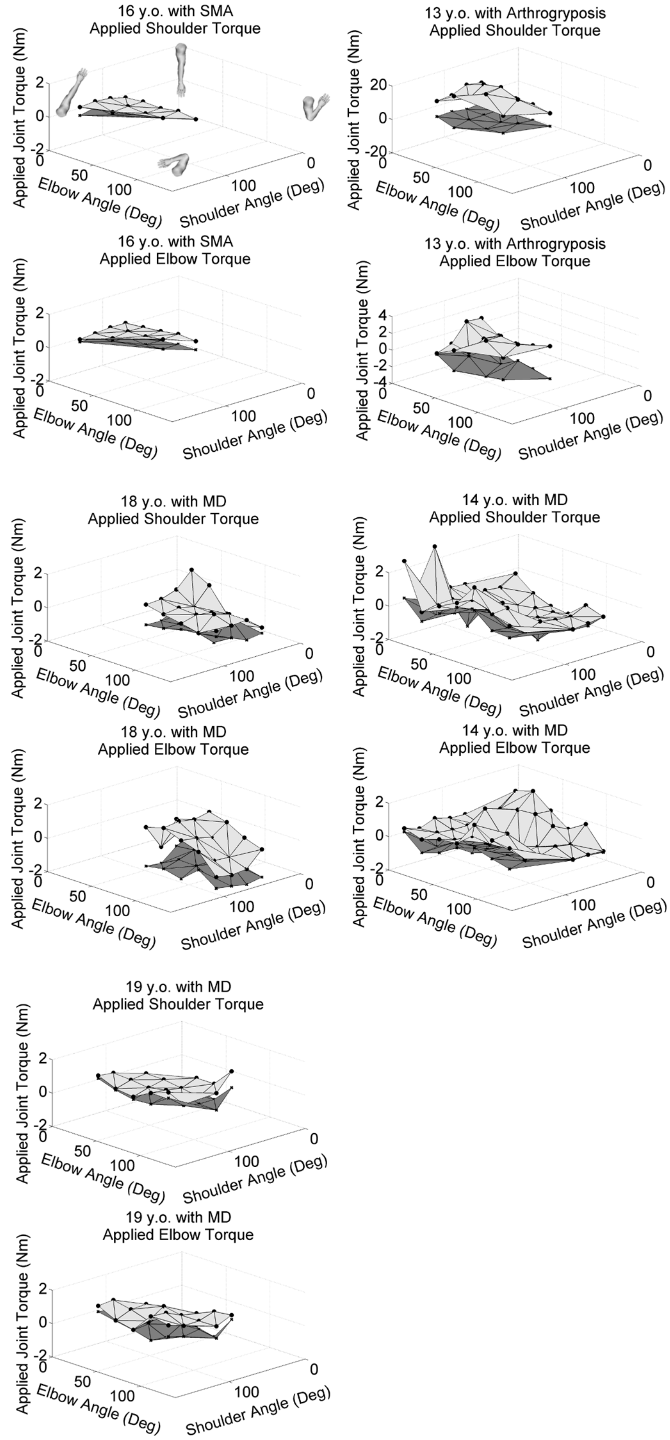

Fig. 8. Maximum applied torque data of children with disabilities. The upper surface is for contracting the arm upwards. The lower surface is for extending the arm downwards.

where τ is the normalized torque fit to the data, q_1 is the shoulder angle and q_2 is the elbow angle in degrees. For each subject, there are two equations. One is for the shoulder and one is for the elbow. The units are dimensionless.

It was also desirable to obtain a map of each disabled subject's maximum upper arm strength throughout the measured range of motion. At each position, the subject with disability was asked to maximally push and pull against the force sensor,

TABLE III
JOINT RANGES, MAXIMUM APPLIED JOINT TORQUES, AND AVERAGE TORQUES FOR CHILDREN WITH DISABILITIES

Subject	Condition	Age	Shoulder Range(deg)	Elbow Range(deg)	Max Shoulder Torque(N/m) [up/down]	Max Elbow Torque(N/m) [up/down]
1	SMA	16	70 - 130	0 - 80	0.13 / 0.43	0.50 / 0.37
2	Arthrogryposis	13	50 - 110	0 - 80	12.7 / 9.71	0.72 / 3.95
3	MD	18	50 - 110	60 - 140	1.68 / 1.08	1.34 / 1.69
4	MD	14	50 - 150	0 - 140	2.76 / 1.94	2.14 / 1.38
5	MD	19	50 - 110	0 - 100	1.41 / 0.63	0.66 / 1.02

while the arm was locked. The direction of push and pull was orthogonal to the force sensor, indicated as the y-axis in Fig. 2. By both pushing and pulling in the y-axis direction, both a negative and positive joint torque would be required, providing a window for each subject's active joint torque strength. For both pushing and pulling, a reading in the sagittal plane was taken from the force sensor. The subjects were given several seconds to rest between readings as the arm position was adjusted to prevent effects of fatigue. The forces obtained while the subject was contracting were transformed into joint torques in the same manner that the passive forces were processed. The passive gravity torques obtained in this study were subtracted from the total applied torques for each position, resulting in the net active torques applied by the human. The net applied torques were sorted into maximum and minimum values and plotted.

III. RESULTS

The full range of data for adults, typical children, and both groups combined are shown in Fig. 4. A 2-D slice of the data is shown in Fig. 5. The left column is the average normalized shoulder torque with the elbow in full extension. The right column is the average normalized elbow torque with the shoulder fixed at 90° from the vertical. The standard deviation is shown in error bars.

The coefficients of the fitted polynomial in (1) for each nondisabled group for the shoulder and elbow joint are shown in Table II. The passive gravity data of children with disabilities are shown in Fig. 6. The values were normalized to the individual's mass and arm length; however, the values were not averaged because of the heterogeneity of the population. A cross section of the passive gravity data is shown in Fig. 7, which also contains the average of typical children for comparison, shown in solid grey. The applied torque data of children with disabilities are shown in Fig. 8. The maximum positive torque is the light surface on top. The maximum negative torque is the dark surface on the bottom. The surfaces between data points are included to help visualization; however, no curve fitting was completed. Table III provides a summary of both shoulder and elbow joint ranges, and maximum voluntary shoulder and elbow joint torques applied by the subject in both directions.

IV. DISCUSSION

For all subjects, the joint torques, as seen in Fig. 5, appear to follow a general pattern similar to a two-link lumped mass model, which is shown as the grey line. This demonstrates that gravity is the dominant component of passive joint torque. However, the elbow curves have the largest deviation from the model curve closer to the joint limits, which reflects increasing joint stiffness. This can be seen for an elbow angle of 0° and 140° in the elbow torque graph of Fig. 5. This is not seen in the graphs for the shoulder, because the measurement device was unable to reach the extreme range of motion of the shoulder. Therefore, the effects of joint stiffness on the shoulder were not as pronounced in this data. From Fig. 4, it can be seen that a third-order polynomial fits the data, and the coefficients for both adults and children have a similar relative magnitude between groups and follow a descending pattern for higher terms. These curves could be used for biomechanical studies and controlling exoskeleton strength amplifiers. To estimate the passive joint torques for a specific individual, the polynomial could be multiplied by the individual's weight and arm length.

For all five disabled subjects, the torque curves as shown in Fig. 7, also exhibited patterns similar to a two-link lumped mass model, indicating gravity is the major component for subjects with disabilities, as well. One thing to note is that all of the subjects with disabilities had a lower range of motion than typically developing children. The 14 year old subject with MD had the greatest range of motion, followed by the subject with arthrogryposis. The other subjects with MD and the subject with SMA had the smallest range. The effects of joint stiffness were much larger than those of typical children and these effects became more noticeable closer to the neutral position in the disabled group. Also, a majority of the curves are above the typically developing children, because many of the subjects had MD and had significantly higher mass on their arms than the group of average children. There are significant differences between different disabilities as seen when comparing different subjects in Figs. 6 and 7, even though all the subjects were users or potential users of the WREX. Even within the MD group, there were significant differences between the different subjects. Since this study was limited to three subjects with MD, it may be possible to determine a pattern for studying a larger group that also considers the progression. A pattern was not discerned from the current study. The passive range of motion of some of the disabled subjects was limited. This prevented us from averaging all the data sets between subjects. This suggests that a subject-specific model will be needed for controlling the powered exoskeleton.

All of the subjects had an absolute maximum applied joint torque of less than 13 Nm for the shoulder joint and 4 Nm for the elbow joint. The maximum applied torque was less than the measured passive gravity torque for each subject, which provides a quantitative estimate of how much assistance these subjects need in upper limb motion. When curling a 17 kg weight, the human can generate on the order of 80 Nm at the elbow, which is far greater than what was measured in the subjects. There was no discernible pattern or shape within or between subjects. As a note, the subjects with the highest maximum applied joint torques were observed to have the greatest upper limb function.

V. Conclusion

In forming a model of a human arm, measurements of the passive joint torques in the sagittal plane showed that a two-link model is inadequate to describe the human arm. It was found that normal adults and children have a similar shape in torque differences that can be represented by a third-degree polynomial. The children with disabilities in this study did not have similar curves and could not be averaged across disabilities. A subject-specific model is suggested. It was also found that the disabled subjects' maximum applied joint torques were lower than the passive gravity torques throughout the measured joint space and were on the order of 5% of normal voluntary torque.

References

[1] T. Rahman, R. Ramanathan, R. Seliktar, and W. Harwin, "A simple technique to passively gravity-balance articulated mechanisms," *J. Mechan. Design* vol. 117, no. 4, p. 655, Dec. 1995.

[2] T. Rahman, W. Sample, R. Seliktar, M. T. Scavina, A. L. Clark, K. Moran, and M. A. Alexander, "Design and testing of a functional arm orthosis in patients with neuromuscular diseases," *IEEE Trans. Neural Syste. Rehabil. Eng.* vol. 15, no. 2, pp. 244–251, Jun. 2007.

[3] W. Maurel, D. Thalmann, P. Hoffmeyer, P. Beylot, P. Gingins, P. Kalra, and M. Thalmann, "A biomechanical musculoskeletal model of human upper limb for dynamic simulation," in *Proc. 5th IEEE EMBS Int. Summer School Biomed. Imag.*, Jun. 2002, p. 16.

[4] S. Williams, R. Schmidt, C. Disselhorst-Klug, and G. Rau, "An upper body model for the kinematical analysis of the joint chain of the human arm," *J. Biomechan.* vol. 39, no. 13, pp. 2419–2429, Jan. 2006.

[5] J. F. Soechting and M. Flanders, "Evaluating an integrated musculoskeletal model of the human arm," *J. Biomechan. Eng.* vol. 119, no. 1, pp. 93–102, Feb. 1997.

[6] C. Carignan, M. Liszka, and S. Roderick, "Design of an arm exoskeleton with scapula motion for shoulder rehabilitation," in *Proc. 12th Int. Conf. Adv. Robot.*, Jul. 2005, pp. 524–531.

[7] J. Perry, J. Rosen, and S. Burns, "Upper-limb powered exoskeleton design," *IEEE/ASME Trans. Mechatronics* vol. 12, no. 4, pp. 408–417, Aug. 2007.

[8] J. Rosen, J. Perry, N. Manning, S. Burns, and B. Hannaford, "The human arm kinematics and dynamics during daily activities—Toward a 7 DOF upper limb powered exoskeleton," in *Proc. IEEE 12th Int. Conf. Adv. Robot.* , Jul. 2005, pp. 532–539.

[9] C. A. Tucker, A. Bagley, K. Wesdock, C. Church, J. Henley, and G. Masiello, "Kinematic modeling of the shoulder complex in tetraplegia," *Topics Spinal Cord Injury Rehabil.* vol. 13, no. 4, pp. 72–85, May 2008.

[10] C. Cornu, F. Goubel, and M. Fardeau, "Muscle and joint elastic properties during elbow flexion in Duchenne muscular dystrophy," *J. Physiol.* vol. 533, no. 2, pp. 605–616, Jun. 2001.

[11] R. Bowen, R. Seliktar, T. Rahman, and M. Alexander, "Surface EMG and motor control of the upper extremity in muscular dystrophy: A pilot study," in *Proc. 23rd Annu. Int. Conf. IEEE EMBS*, 2001, vol. 2, pp. 1220–1223.

[12] S. Armand, M. Mercier, E. Watelain, K. Patte, J. Pelissier, and F. Rivier, "A comparison of gait in spinal muscular atrophy, type II and Duchenne muscular dystrophy," *Gait Posture* vol. 21, no. 4, pp. 369–378, Jun. 2005.

[13] J. Sunnegårdh, L. E. Bratteby, L. Nordesjö, and B. Nordgren, "Isometric and isokinetic muscle strength, anthropometry and physical activity in 8 and 13 year old Swedish children," *Eur. J. Appl. Physiol. Occupat. Physiol.* vol. 58, no. 3, pp. 291–297, 1988.

[14] S. Mathur, D. J. Lott, C. Senesac, S. A. Germain, R. S. Vohra, H. L. Sweeney, G. A. Walter, and K. Vandenborne, "Age-related differences in lower-limb muscle cross-sectional area and torque production in boys with Duchenne muscular dystrophy," *Arch. Phys. Med. Rehabil.* vol. 91, no. 7, pp. 1051–1058, Jul. 2010.

[15] D. Winter, *Biomechanics and Motor Control of Human Movement*, 3rd ed. New York: Wiley, 2005.

Daniel Ragonesi received the BSME degree with high honors in engineering from Grove City College, Grove City, PA, USA, in 2008. He is currently working toward the Ph.D. degree in mechanical engineering on a powered, upper-limb orthosis for the pediatric population at the at the University of Delaware, Newark, DE, USA.

He joined the Mechanical Systems Lab and Robotics Rehabilitation Lab at the University of Delaware, as well as, the Pediatric Engineering Research Lab at the Alfred. I. DuPont Hospital for Children in Wilmington, DE, USA, as a Research Assistant.

Mr. Ragonesi was awarded the graduate achievement award from the University of Delaware in 2009 for outstanding research and contribution to the department.

Sunil K. Agrawal (M'92) received the Ph.D. degree in mechanical engineering from Stanford University, Stanford, CA, USA, in 1990.

He is currently a Professor with the Department of Mechanical Engineering, Columbia University, New York. He has authored more than 325 journal and conference papers and two books in the areas of controlled mechanical systems, dynamic optimization, and robotics.

Dr. Agrawal is a Fellow of the American Society of Mechanical Engineers (ASME). He received a Presidential Faculty Fellowship from the White House in 1994, a Bessel Prize at Germany in 2003, and a Humboldt U.S. Senior Scientist Award in 2007. He has been an editorial board member of several journals published by ASME and IEEE.

Whitney Sample received the B.F.A. degree in industrial design from Carnegie Mellon University, Pittsburgh, PA, USA, in 1987.

He is a Research Design Engineer at the Alfred I. duPont Hospital for Children. His 25-year career in the service of people with disabilities began at The Center for Human Service Robotics at Carnegie Mellon. For nearly five years, he led the design and development of several rehabilitation robotics projects. In 1990, he worked as a robotics design consultant to Walt Disney Imagineers.

Tariq Rahman received the Ph.D. degree from Drexel University, Philadelphia, PA, USA, in 1990.

He then joined the Alfred I. duPont Hospital for Children as a post-doctoral fellow working on assessment of rehabilitation robotics and incorporated prosthetic ideas of extended physiological proprioception into rehabilitation robotics. He is currently a Senior Research Engineer at the hospital and Director of the Center for Orthopedics Research and Development. He also holds the position of Research Associate Professor in the School for Biomedical Engineering at Drexel University and Research Professor in mechanical Engineering at University of Delaware. He has published extensively in the area of rehabilitation engineering on issues relating to tremor reduction, robotics, orthotics, and orthopedics. He holds numerous patents related to technology for people with disabilities.